Scientific Research Publishing

Open Journal of Applied Sciences, 2026, 16(4), 1360-1385
https://www.scirp.org/journal/ojapps
ISSN Online: 2165-3925
ISSN Print: 2165-3917

Analysis and Modeling of Energy Losses in an Electrical Power System Using Maxwell's Equations

Anthony Bassesuka Sandoka Nzao[1*], Vunda Ngulumingi Christian[1], Tuka Biaba Samuel Garcia[2]

[1]Department of Electrical Engineering, ISTA Kinshasa, Kinshasa, Democratic Republic of the Congo
[2]Doctoral School of ISTA Kinshasa, Complementary Master in Science and Technology/Electrical Engineering, Electrotechnical Option, Kinshasa, Democratic Republic of Congo
Email: *bass_sandoka@yahoo.fr, christianvunda1@gmail.com, tukasamuel23@gmail.com

How to cite this paper: Nzao, A.B.S., Christian, V.N. and Garcia, T.B.S. (2026) Analysis and Modeling of Energy Losses in an Electrical Power System Using Maxwell's Equations. *Open Journal of Applied Sciences*, **16**, 1360-1385.
https://doi.org/10.4236/ojapps.2026.164079

Received: March 2, 2026
Accepted: April 27, 2026
Published: April 30, 2026

Abstract

The consequences of energy losses in a three-phase electrical system include increased heat loss in conductors, causing overheating of cables and equipment, which can lead to fires or voltage drops. This reduces motor efficiency, increases operating costs, and can degrade power quality, causing failures in other equipment connected to the grid. In the long term, this shortens equipment lifespan and can cause cascading grid degradation. These energy losses in three-phase electrical systems, such as power grids, are categorised into two types: technical losses and non-technical losses. Non-technical losses represent energy consumed but not recorded. Technical losses refer to the losses in the grid resulting from Joule heating, corona discharge, and iron losses in transformers. Evaluating energy losses in a high-voltage (HV) three-phase electrical system allows for optimizing grid performance, increasing transmission efficiency, and reducing operating costs. It helps to reduce voltage drops, increase available power, and minimize energy waste, thus limiting the risks of failure and accidents. This article aims to apply a method based on Maxwell's equations for the analysis and modeling of energy losses in a power system, specifically in the case of high-voltage AC transmission lines. The Simulink model, developed in MATLAB using experimental data from the 262 km long 220 kV Inga-Kinshasa high-voltage AC line in the Democratic Republic of Congo, was compared to the results of a proposed model for the analysis and modeling of energy losses in high-voltage AC transmission lines. The results of the various 2D simulations obtained show that the analytical approaches and the computer tools used are satisfactory.

Keywords

Power Electrical System, HV-AC Power Transmission Lines, Energy Losses,

Technical Losses, Non-Technical Losses, Voltage Drop, Joule Effect, Analysis, Modeling, Maxwell's Equations, 2D Simulations, Matlab/Simulink

1. Introduction

The transmission of electrical energy through various elements of an electrical network results in energy losses. These losses in electrical networks are divided into two categories: technical losses and non-technical losses. Non-technical losses represent energy consumed but not recorded [1]-[3]. Technical losses correspond to losses in the networks due to Joule heating (heating of cables), corona discharge (electrical discharge caused by ionization of the medium surrounding a conductor), and iron losses from transformers [3]-[4].

Technical losses in the electrical network are losses of energy dissipated as heat during transmission and distribution. These losses are a concern for stakeholders in the sector because they need to be compensated [3]-[5]. The cost of these losses is either passed on to consumers or borne by network operators, who must anticipate the volume and purchase the corresponding electricity to meet demand [3]-[8].

According to existing literature [9] [10], technical losses in electrical grids lead to increased operating costs and higher energy consumption [11], resulting in reduced profitability for distributors and potentially higher prices for consumers [12] [13]. These losses, caused by the Joule effect (cable heating), the corona effect, and transformer losses, reduce the overall efficiency of the grid [14] [15]. Furthermore, they can cause grid stability problems and, in extreme cases, lead to widespread outages [16] [17]. These losses result, among other things, in voltage drops.

Assessing energy losses is crucial for the financial and technical performance of electrical grids. It allows for measuring grid efficiency, identifying the causes of losses (such as the Joule effect or load imbalances), and reducing costs by preventing overproduction. Furthermore, a sound assessment helps to control the supply-demand balance, optimize investments, and better distinguish technical losses from non-technical losses (fraud, metering errors) [18].

According to [9] [10], the energy loss rate, the ratio of energy lost to total energy injected, is an internationally recognised indicator relevant for assessing the performance of electricity grids and the companies responsible for their operation [11]-[14].

Methods for analyzing and modeling energy losses in a high-voltage electrical network include deterministic and statistical approaches. Deterministic methods (energy balance by voltage level and evaluation of technical energy losses inherent in the physical operation of networks [15] [16]) use calculations based on physics (Joule effect, corona effect, transformer losses), while statistical methods rely on historical data to estimate losses and are often used for medium- and long-term forecasts. These two approaches can be combined, for example, by calibrating statistical forecasts with physical measurements or energy balances. The energy bal-

ance will determine the total energy lost and the technical losses; by subtracting the total energy lost from the technical losses, non-technical losses will be assessed [16] [17].

Deterministic methods have the advantage of offering high accuracy if the data are precise, but they can be rigid and fail to handle uncertainties [18] [19], as fraudulently siphoned electrical energy, considered non-technical losses, is not taken into account. Statistical methods are more flexible and allow for the management of variations, but they can be less precise and struggle to estimate exact energy volumes, sometimes reproducing atypical past events [20].

This manuscript proposes a method for analyzing and modeling energy losses in an electrical system, based on Maxwell's equations, which provide a theoretical framework for understanding these losses. In the absence of non-technical losses, the voltage drop is correlated with technical losses. Maxwell's equations allow for the estimation of energy losses in high-voltage lines using an analytical model based on two measurements: the voltage drop at a given time (t) and the power factor under normal network conditions. This method requires simultaneous voltage readings at the starting and ending nodes. Calculating averages over fixed time horizons necessitates a computer network due to the distances between the nodes. The advantage of this approach compared to existing ones in the literature lies in its ease of implementation and its implicit consideration of fraudulently consumed electrical energy, considered as non-technical losses, since it is included in the losses calculated from the known voltage drop at a given instant (t).

The results obtained show a direct correlation between the proposed models and the Simulink models developed in MATLAB.

2. Method

The analysis and modeling of energy losses in a three-phase electrical system using Maxwell's equations are based on the study of electromagnetic fields and their interactions to deduce the losses [21]-[23]. Maxwell's equations (Expressions 1 - 7), in their differential form, describe the sources (charges and currents) and the evolution of the electric ($\boldsymbol{E}$) and magnetic ($\boldsymbol{B}$) fields [24] [25]. The losses manifest themselves as heat due to the Joule effect in the conductors $(\boldsymbol{j}, \boldsymbol{E})$, eddy currents in the ferromagnetic cores (related to the variation of the magnetic field), and magnetic losses in the ferromagnetic materials, modelled via relationships derived from these equations [26] [27]. The scope of this article concerns technical losses due to the Joule effect in the conductors of high-voltage AC lines.

2.1. Assumptions and Applicability

The main simplifications used in this article are:

- Balanced currents.
- Constant power factor.
- Negligible transverse parameters.
- Invariant line parameters.

The model is susceptible to failures (e.g., compensation devices, tap changes, unbalanced load).

2.2. Modeling of High-Voltage Power Lines

Modelling power lines allows us to represent their expected electrical behaviour. The main modelling method is based on a system of two partial differential equations that describe the evolution of voltage and current on a power line as a function of distance and time. Two methods, with completely distinct foundations, are used:

- Field theory, developed from Maxwell's equations [23], is rigorous but not always easy to apply and allows us to establish the second theory (circuit theory).
- Circuit theory: modelling propagation along the line by constructing an equivalent circuit (inductors, capacitors, resistors), the analysis of which is simple.

In this article, we will limit ourselves to field theory. Indeed, field theory, developed from Maxwell's equations [27], is rigorous but not always easy to apply and allows us to establish the second theory (circuit theory). At any point in space, which is not located on a surface separating two media, that is, in a linear, homogeneous, and isotropic (LHI) medium, Maxwell's general equations specify that [28]:

$$\nabla \times \boldsymbol{E}(t,r) = -\frac{\partial \boldsymbol{B}(t,r)}{\partial t} \tag{1}$$

$$\nabla \times \boldsymbol{H}(t,r) = \boldsymbol{J}(t,r) + \varepsilon_0 \frac{\partial \boldsymbol{E}(t,r)}{\partial t} \tag{2}$$

$$\nabla \cdot \boldsymbol{D}(t,r) = \rho(t,r) \tag{3}$$

$$\nabla \cdot \boldsymbol{B}(t,r) = 0 \tag{4}$$

The basic variables of these equations are:

$\boldsymbol{B}$: Magnetic induction (Tesla, T).

$\boldsymbol{H}$: Magnetic field strength (Ampere/meter^2, Am^{-2}).

$\boldsymbol{D}$: Electric flux density (coulomb/meter^2, Cm^{-2}).

$\boldsymbol{E}$: Electric field density (volt/meter, Vm^{-1}).

$\boldsymbol{J}$: Electric current density (Ampere/meter^2, Am^{-2}).

ρ: Electric charge density (coulomb/meter^3, Cm^{-3}).

With:

$$\boldsymbol{B} = \mu \boldsymbol{H} \tag{5}$$

$$\boldsymbol{D} = \varepsilon \boldsymbol{E} \tag{6}$$

$$\boldsymbol{J} = \sigma \boldsymbol{E} \tag{7}$$

And:

μ: Magnetic permeability in Tm^2/A

ε: Electrical permeability in Cm^{-3}/V

σ: Electrical conductivity

In this form, called local or differential, Maxwell's equations express relationships between spatial variations of certain fields and temporal variations of other fields [26] [27].

In a vacuum:

$$\boldsymbol{B}(t,r)=\mu_0\boldsymbol{H}(t,r) \tag{8}$$

$$\boldsymbol{D}(t,r)=\varepsilon_0\boldsymbol{E}(t,r) \tag{9}$$

Then Maxwell's equations become [26] [27]:

$$\nabla\times\boldsymbol{H}(t,r)=\varepsilon_0\frac{\partial\boldsymbol{E}(t,r)}{\partial t} \tag{10}$$

$$\nabla\cdot\boldsymbol{H}(t,r)=0 \tag{11}$$

$$\nabla\cdot\boldsymbol{B}(t,r)=0 \tag{12}$$

The differential operator $\nabla\cdot$ is used to express the curl operation $\nabla\times$ = rot and the divergence operation $\nabla\cdot=\mathrm{div}$. Maxwell's equations can also be expressed in "global form" as follows [26] [27]:

$$\oint_c\boldsymbol{E}(t,r)\mathrm{d}\boldsymbol{l}=-\int_s\boldsymbol{n}\frac{\partial\boldsymbol{B}(t,r)}{\partial t}\mathrm{d}A \tag{13}$$

$$\oint_c\boldsymbol{H}(t,r)\mathrm{d}\boldsymbol{l}=-\int_s\boldsymbol{n}\left(\frac{\partial\boldsymbol{D}(t,r)}{\partial t}+\boldsymbol{J}(t,r)\right)\mathrm{d}A \tag{14}$$

After integrating Equations (13) and (14), using the divergence theorem, the two Equations (4) and (6) then become [26] [27]:

$$\oint_c\boldsymbol{n}\boldsymbol{D}(t,r)\mathrm{d}A=\int_v\rho(t,r)\mathrm{d}A \tag{15}$$

$$\int_s\boldsymbol{n}\boldsymbol{B}(t,r)\mathrm{d}A=0 \tag{16}$$

The boundary conditions for fields [26] [27] are:

$$\boldsymbol{n}\times\left[\boldsymbol{E}_1(t,r)-\boldsymbol{E}_2(t,r)\right]=0 \tag{17}$$

$$\boldsymbol{n}\times\left[\boldsymbol{H}_1(t,r)-\boldsymbol{H}_2(t,r)\right]=\boldsymbol{j}_s \tag{18}$$

$$\boldsymbol{n}\times\left[\boldsymbol{D}_1(t,r)-\boldsymbol{D}_2(t,r)\right]=\rho_s \tag{19}$$

$$\boldsymbol{n}\times\left[\boldsymbol{B}_1(t,r)-\boldsymbol{B}_2(t,r)\right]=0 \tag{20}$$

With:

$\boldsymbol{n}$: is the normal to the separation surface, going from medium 2 to medium 1;

$\boldsymbol{J}_s$: is the surface current density;

ρ_s : is the surface charge density.

2.3. Pi Modeling of High Voltage AC Power Lines

Pi modelling of power lines (see **Figure 1** below) allows us to represent their expected electrical behaviour. It is based on the telegraphers' equations [28]-[30].

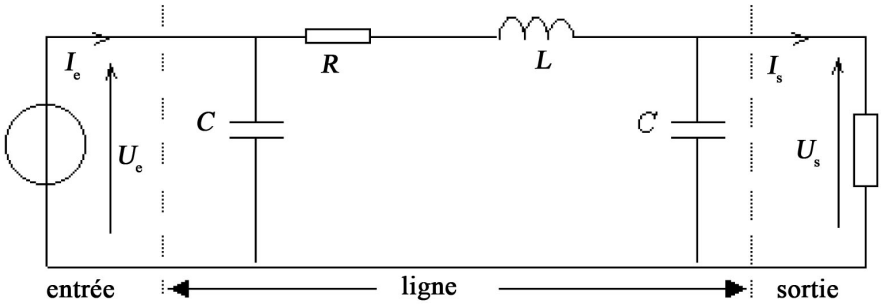

Figure 1. Simplified model of a high-voltage power line [28]-[30].

A portion of a power line can be represented by the four-terminal network in **Figure 2** below, where [31]-[35]:

- The linear resistance (per unit length) R of the conductor is represented by a series resistance (expressed in ohms per unit length).
- The linear inductance L is represented by an inductance (Henry per unit length).
- The linear capacitance C between the two conductors is represented by a shunt capacitor C (Farad per unit length).
- The linear conductance G of the dielectric medium separating the two conductors is represented by a shunt resistance (Siemens per unit length). The resistance in this model has a value of $1/G$ Ohms.

In this model, we define the voltage at any point a distance x from the beginning of the line and at any time t, the voltage $U(x,t)$ and the current $I(x,t)$. The equations are written [36]-[40]:

$$\begin{cases} \dfrac{\partial U}{\partial x}(x,t) = -L\dfrac{\partial I}{\partial t}(x,t) - RI(x,t) \\ \dfrac{\partial I}{\partial x}(x,t) = -C\dfrac{\partial U}{\partial t}(x,t) - GU(x,t) \end{cases} \tag{21}$$

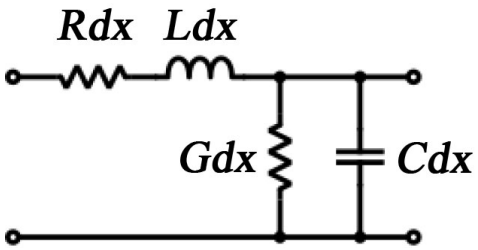

Figure 2. Two-port network model of a high-voltage power line [36]-[40].

From the formulation above, we can derive two partial differential equations, each involving only one variable [36]-[40]:

$$\begin{cases} \dfrac{\partial^2 U}{\partial x^2}(x,t) = LC\dfrac{\partial^2 U}{\partial t^2}(x,t) + (RC+GL)\dfrac{\partial U}{\partial t}(x,t) + GRU(x,t) \\ \dfrac{\partial^2 I}{\partial x^2}(x,t) = LC\dfrac{\partial^2 I}{\partial t^2}(x,t) + (RC+GL)\dfrac{\partial I}{\partial t}(x,t) + GRI(x,t) \end{cases} \tag{22}$$

2.4. High-Voltage Line Parameter Models

The calculation of the electrical parameters used for the modelling is based on Maxwell's equations. The model with a single Pi section is only valid for low frequencies and short power lines; otherwise, several Pi sections must be connected in series [34]-[37].

2.4.1. Resistance Model

Starting from the local Ohm's law in local form [40]:

$$\boldsymbol{j} = \delta \cdot \boldsymbol{E} \tag{23}$$

Or:

$\boldsymbol{J}$: Current density (A/m^2)

δ : Electrical conductivity (Ω^{-1})

$\boldsymbol{E}$: The electric field (V/m)

The resistance of conductors depends on temperature and frequency; it is defined by [39] [40]:

$$R = \frac{l}{GS} = \frac{\rho l}{s}(\Omega) \tag{24}$$

The resistivity of a material increases with temperature according to this law.

$$\rho = \rho_o\left(1 + \alpha\Delta t\right) \tag{25}$$

Or:

α : The coefficient of dilation

Δt : Temperature variation ˚C

ρ_o : is the resistivity of the conductor at 20˚C (Ωm)

$$R = \frac{\rho_o\left(1 + \alpha\Delta t\right)l}{s}(\Omega) \tag{26}$$

2.4.2. Inductance Model

A conductor carrying a varying current "I" generates a magnetic flux "φ". The variation of this flux is the cause of the appearance of the induced voltage. To account for these effects, the linear inductance of a conductor alone is defined as follows [36]-[40]:

$$L = \frac{\varphi}{I} = \frac{\mu_0}{2\pi}\left(\ln\frac{2h}{D} + \frac{1}{4n}\right) \tag{27}$$

With: h (m): height of the line relative to the ground. D (mm): diameter of the conductor. n: Number of conductors in the bundle [36]-[40].

2.4.3. Capacity Model

The electric field established between the line and ground is the cause of the appearance of capacitive current (leakage current). To account for these effects, capacitance is defined as follows [36]-[40]:

$$C = \frac{Q}{v} = \frac{2\pi\varepsilon_0}{\ln\frac{D}{h}} \tag{28}$$

2.5. Modeling of Energy Losses in High-Voltage Lines

For the calculations of losses in the lines, we assume that the current intensities are balanced in the lines; that is, we start from the assumption of equipartition of the loads in the lines. Energy *losses* in HV lines are intrinsically linked to Maxwell's equations, in particular via Poynting's theorem, which describes the electromagnetic energy balance. The term for dissipation due to the Joule effect appears in the local energy conservation equation.

The starting point is Poynting's theorem in its local form, derived from Maxwell's equations (notably Maxwell-Faraday and Maxwell-Ampère) [36]-[40]:

$$\nabla \cdot \Pi + \frac{\partial \varpi_{em}}{\partial t} + P_j = 0 \tag{29}$$

$$\Pi = \frac{1}{\mu_0}\left(\boldsymbol{E} \wedge \boldsymbol{B}\right) \tag{30}$$

$$\varpi_{em} = \frac{1}{2}\left(\varepsilon_0 \boldsymbol{E} + \frac{1}{\mu_0}\boldsymbol{B}^2\right) \tag{31}$$

With: Π is the Poynting vector (surface density of electromagnetic power). ϖ_{em} is the volumetric density of stored electromagnetic energy. P_j is the volumetric density of power dissipated by Joule effect.

By combining Maxwell's equations, we can isolate the dissipation term. For a conducting medium obeying local Ohm's law ($J = \rho E$), where ρ is the electrical conductivity, the volumetric power density dissipated by Joule heating is given by:

$$P_j = \boldsymbol{E} \cdot \boldsymbol{j} \tag{32}$$

Using Ohm's law, it can be expressed as a function of the electric field or current density:

$$P_j = \sigma E^2 = \frac{1}{\sigma} J^2 \tag{33}$$

To obtain the total power dissipated by Joule heating in a given volume V (for example, a conductor of resistance R), the volumetric power density must be integrated over this volume:

$$P_p = \iiint_v P_j \mathrm{d}v = \iiint_v \boldsymbol{E} \cdot \boldsymbol{j} \mathrm{d}v \tag{34}$$

This integration leads, in the simple case of an Ohmic circuit, to the well-known macroscopic law:

$$P_p = RI^2 \tag{35}$$

For a high-voltage line of L_c = conductor length, containing n conductors of the line and R_c = linear resistance, carrying the maximum current Imax, the Joule effect losses in this line are calculated using the following equation:

$$P_j = n\left(R_c I_{\max}^2 L_c\right)[\mathrm{W}] \tag{36}$$

With:

P_j = Joule effect losses in lines

n = Number of conductors on the line

R_c = Linear resistance [Ω/km]

$I_{\max}$ = Maximum current of a conductor [A]

L_c = Length of conductor [m]

These losses are obtained primarily based on the physical characteristics of the line. Given the line voltage and the current it can carry, the active power that the line will supply can perhaps be modelled as follows [41]:

$$P = \sqrt{3} U_L I_{\max} \cos\varphi \left[\text{kW}\right] \tag{37}$$

With:

- ✓ P = Active power supplied by the line;
- ✓ U_L = Line voltage [kV];
- ✓ $I_{\max}$ = intensity of a conductor [A];
- ✓ $\cos\varphi = 0.9$

We know that in a conductor, the power lost due to Joule heating is "$R_c I_c^2$", with "I_c", the current flowing in the conductor. Considering the balanced, three-phase line, the apparent power it carries will be written as follows [42]:

$$S = \sqrt{3} U_L I_L = \sqrt{P^2 + Q^2} \tag{38}$$

With:

U_L = Line voltage (kV)

I_L = Line intensity (A)

P = Active power carried by the line (W)

Q = reactive power carried by the line (VAr)

Consider the following equality:

$$3U_L^2 I_L^2 = P^2 + Q^2 \tag{39}$$

Thus we can draw the line current I_L:

$$I_L^2 = \frac{P^2 + Q^2}{3U_L^2} \tag{40}$$

The power loss "P_P" in the line can thus be noted as:

$$P_P = 3R_L I_L^2 \tag{41}$$

Substituting expression (40) into relation (41) gives us:

$$P_P = 3R_L I_L^2 = 3R_L \left(\frac{P^2 + Q^2}{3U_L^2} \right) \tag{42}$$

$$P_P = R_L \left(\frac{P^2 + Q^2}{U_L^2} \right) = R_L \frac{P^2}{U_L^2} + R_L \frac{Q^2}{U_L^2} \tag{43}$$

With: R_L, I_L and U_L, respectively the line resistance, the maximum line current and the line voltage.

The relative losses in the line are thus given by the following expression:

$$P_{pr} = \frac{3R_L I_L^2}{\sqrt{3} U_L I_L \cos\varphi} \tag{44}$$

With:

- ✓ P_{pr} : Relative power losses in %;
- ✓ I_L : Line intensity in A;
- ✓ R_L : Conductor resistance in Ω;
- ✓ U_L : Voltage composed of a V-shaped line.

2.6. Modeling of the Relative Voltage Drop in the HV Line

The assumptions for calculating the voltage drop in AC for a high-voltage AC line are that the overvoltage is primarily caused by the longitudinal parameters, resistance and reactance in series (R_L, X_L), and that the contribution of the transverse parameters is negligible. The transmission line model adopted is therefore the equivalent circuit shown in Figure 3 below [43] [44]:

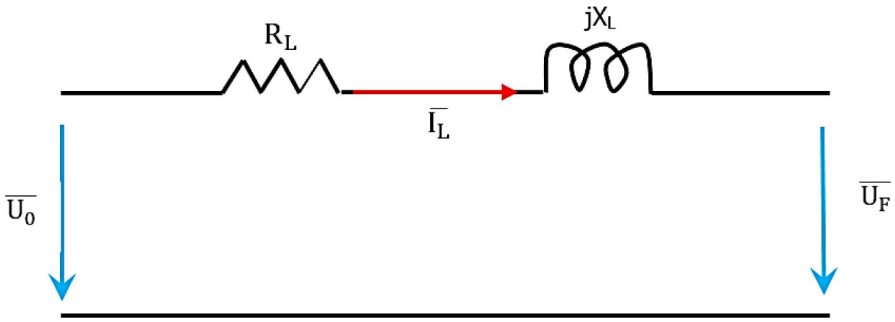

Figure 3. Equivalent circuit of the HV line [43]-[47].

Legend

$\overline{U_O}$ =Voltage from the origin relative to neutral in kV

$\overline{I_L}$ =Maximum line intensity at A

$\overline{U_F}$ =Voltage at the end relative to neutral in kV

X_L = Reactance inductance of the line in Ω

R_L =Line resistance in Ω

Applying Kirchhoff's law to Figure 3 above, we find the following equations:

$$\overline{U_O} = X_L \overline{I_L} + R_L \overline{I_L} + \overline{U_F} \tag{45}$$

$$\overline{U_O} - \overline{U_F} = \left(R_L + X_L\right)\overline{I_L} \tag{46}$$

$$\Delta_U = \left|\overline{U_O}\right| - \left|\overline{U_F}\right| \approx R_L I_L \cos\varphi + X_L I_L \sin\varphi \tag{47}$$

Thus, the relative phase-to-neutral voltage drop can be denoted by the following equation:

$$\Delta U_r = \frac{\Delta_U}{U_L} \tag{48}$$

Integrating Equation (47) into expression (48), we find the following equations:

$$\frac{\Delta_U}{U_L} = \frac{R_L I_L \cos\varphi}{U_L} + \frac{X_L I_L \sin\varphi}{U_L} \tag{49}$$

$$\frac{\Delta_U}{U_L} = \frac{R_L U_L I_L \cos\varphi}{U_L^2} + \frac{X_L U_L I_L \sin\varphi}{U_L^2} \tag{50}$$

Multiplying the right-hand side of Equation (50) by $\sqrt{3}$, the voltage drop relative to the line voltage gives:

$$\Delta U_r = \frac{R_L \sqrt{3} U_L I_L \cos\varphi}{U_L^2} + \frac{X_L \sqrt{3} U_L I_L \sin\varphi}{U_L^2} \tag{51}$$

We know that in three-phase:

$$P = \sqrt{3} U_L I_L \cos\varphi \tag{52}$$

$$Q = \sqrt{3} U_L I_L \sin\varphi \tag{53}$$

Thus, expressions (52) and (53) in relation (51) give us:

$$\Delta U_r = \frac{R_L P}{U_L^2} + \frac{X_L Q}{U_L^2} \tag{54}$$

Let's highlight R_L in Equation (54), so we find:

$$\Delta U_r = \frac{R_L}{U_L^2}\left(P + \frac{X_L}{R_L} Q\right) \tag{55}$$

Therefore, $\frac{Q}{P} = \text{tg}\varphi$ in expression (55), we find:

$$\Delta U_r = \frac{R_L}{U_L^2} P\left(1 + \frac{X_L}{R_L}\text{tg}\varphi\right) \tag{56}$$

$$\Delta U_r = \frac{\sqrt{3} R_L U_L I_L \cos\varphi}{U_L^2}\left(1 + \frac{X_L}{R_L}\text{tg}\varphi\right) \tag{57}$$

2.7. Modeling of Energy Losses in High-Voltage Lines Depending on the Relative Voltage Drop

Since losses result, among other things, in voltage drop, we can determine the models that highlight the losses related to the active power transmitted by the line and the voltage drop related to the line voltage, based on expressions (44) and (57). The ratio between P_{pr} these two values ΔU_r gives:

$$\frac{P_{pr}}{\Delta U_r} = \frac{\dfrac{3 R_L I_L^2}{\sqrt{3} U_L I_L \cos\varphi}}{\dfrac{\sqrt{3} R_L U_L I_L \cos\varphi}{U_L^2}\left(1 + \dfrac{X_L}{R_L}\text{tg}\varphi\right)} \tag{58}$$

Hence:

$$P_{pr} = \frac{\Delta U_r}{\cos^2\varphi\left(1 + \dfrac{X_L}{R_L}\text{tg}\varphi\right)} \tag{59}$$

From this relation (59), we can draw the following conclusions:

$$\text{Low voltage} \quad X_L = 0 \quad P_{pr} = \frac{\Delta U_r}{\cos^2 \varphi} \tag{60}$$

$$\text{Medium voltage} \quad X_L \cong R_L \quad P_{pr} = \frac{\Delta U_r}{\cos\varphi\left(\cos\varphi + \sin\varphi\right)} \tag{61}$$

$$\text{High Voltage} \quad X_L \neq R_L \quad P_{pr} = \frac{\Delta U_r}{\cos^2 \varphi\left(1 + \frac{X_L}{R_L}\text{tg}\varphi\right)} \tag{62}$$

$\frac{X_L}{R_L} = \text{tg}\delta$ The quality factor of a high-voltage (HV) line is typically between 2 and 10 for a 220 kV HV line. $\text{tg}\delta$ It is calculated based on the linear inductance (L) and resistance (R), which are low over long distances. The quality factor of an HV power line is not a standard value, but rather the result of calculations based on its physical properties (inductance, resistance, capacitance) and the line frequency.

$$P_{pr} = \frac{\Delta U_r}{\cos^2 \varphi\left(1 + \text{tg}\delta \cdot \text{tg}\varphi\right)} \tag{63}$$

The $\text{tg}\delta = 2$, losses related to the active power transmitted by the HV line as a function of the voltage drop relative to the line voltage are quantified from expression (64) below:

$$P_{pr} = \frac{\Delta U_r}{\cos^2 \varphi\left(1 + 2 \cdot \text{tg}\varphi\right)} \tag{64}$$

2.8. Accurate and Reproducible Description of the Use of High Voltage (HV) Line Data

To provide an accurate and reproducible description of the use of data from the SNEL Inga-Kinshasa HV line in a calculation or simulation model, the following are the standard parameters generally applied in engineering studies of the Congolese grid:

2.8.1. Dataset Description

- **Source**: SNEL (National Electricity Company) SCADA System.
- **Measurement Points**:
  - Transmitting End: Inga substations (Inga 1 or Inga 2).
  - Receiving End: Kimwenza substations (depending on the specific line of the corridor).
  - Parameters Collected: Line Voltage (U), Phase Current (I), Active Power (P), Reactive Power (Q), and Frequency (f).

2.8.2. Processing Protocol (Model)

- Sampling Interval: Typically 10 seconds for SCADA historical archiving, although phase measurement units (PMUs), if present, can reach 50 - 60 samples per second.

- Averaging Window: Raw data is often integrated over a 10 - 15 minute window for load planning studies, or stored at the second level for transient stability analyses.
- Operating Conditions: Steady State for power flows. Data generally excludes periods of major maintenance unless the study focuses on reliability.
- Preprocessing:
- Filtering of outliers due to telecommunication errors.
- Normalization (per unit conversion) based on nominal voltages (220 kV depending on the segment).

2.8.3. Assumptions of Uncertainty and Accuracy

In the absence of specific calibration certificates, the models use the following industry standards for high-voltage sensors:

a) Voltage Measurements (TP):

- Accuracy class: 0.5% to 1%.
- Allowable uncertainty: ±1% (including transmission line errors).

b) Current Measurements (TI):

- Accuracy class: 0.5% (measurement) or 5P20 (protection).
- Allowable uncertainty: ±1.5% at full scale.

c) Power (P and Q):

- The combined uncertainty is generally estimated at ±2% to ±3%.

2.8.4. Use in the Model

The data is primarily used for:

- Validation: Adjusting the line parameters (impedance, admittance) so that the software results (Matlab) correspond to the actual measurements.
- State Estimation: Verify the consistency of redundant measurements between Inga and Kinshasa to identify actual line losses.

3. Simulation

3.1. Declaration of High-Voltage Line Parameters

The numerical values of the HV line parameters, such as $R_L = 0.07$ Ω/km, $X_L = 0.15$ Ω/km, line length 262 km, power factor $\cos\varphi = 0.9$, $\text{tg}\varphi = 0.484$, and respective active and reactive power ($P = 350$ MW and $Q = 169.4$ MVAr the line input) and ($P = 279$ MW and $Q = 84.1$ MVAr the line output), are taken from SNEL/DRC.

3.2. Simulation Results

Energy losses are a major concern for all producers, transmission, and distribution of electrical energy. To simulate these losses in high-voltage lines, we assumed that the current intensities were balanced. Considering the proposed models (see Equations (57) and (64)), the computer tools used, the characteristic data of the 220 kV line, and the power transmission readings provided by SNEL/DG/PKB, the simulation results are presented in **Figures 4-20** below:

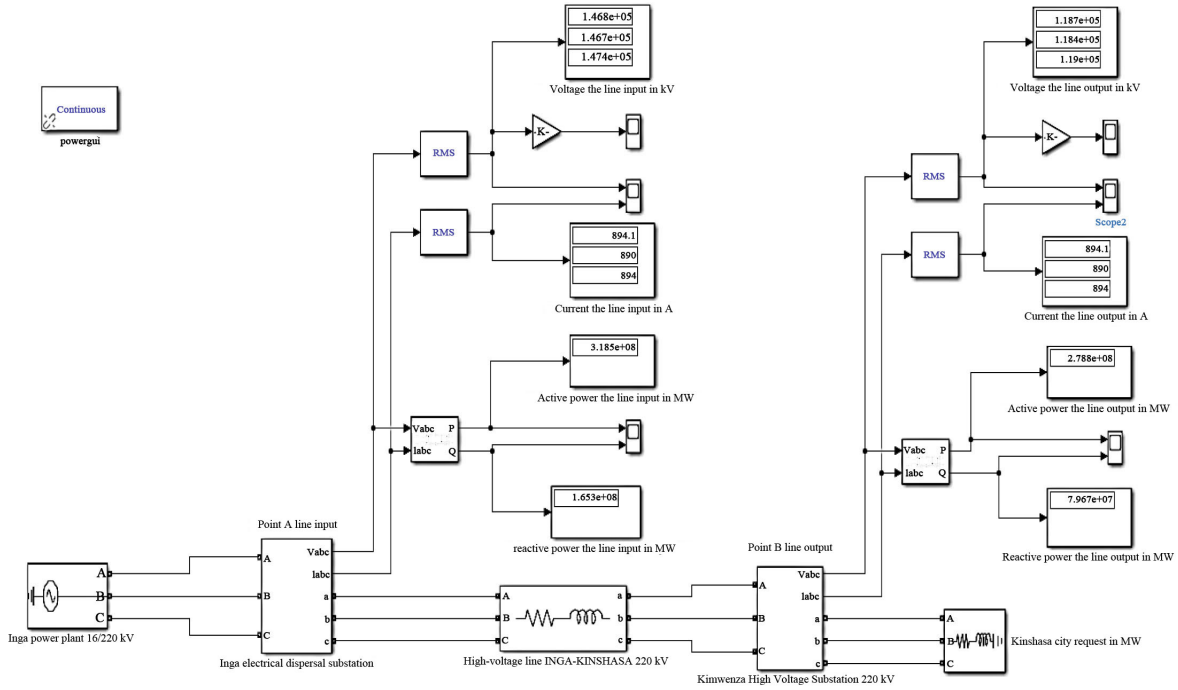

Figure 4. Simulink model of power transmission on the 220 kV Inga-Kimwenza high-voltage line.

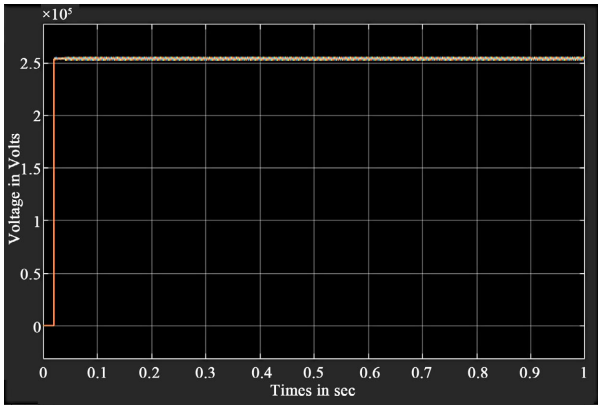

Figure 5. Voltage of point A the Inga dispersal substation (220 kV HV line input) in Volts.

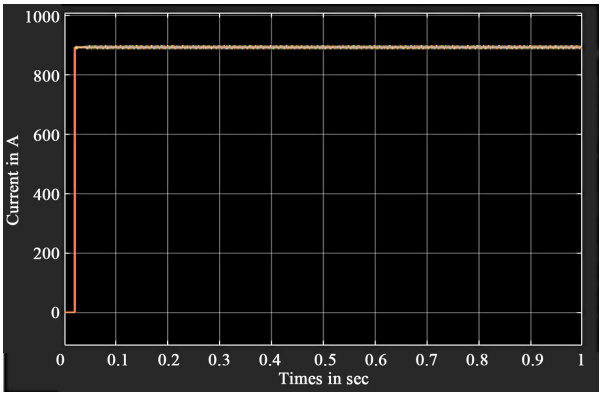

Figure 6. Current of point A the Inga dispersal substation (220 kV HV line input) in Amperes.

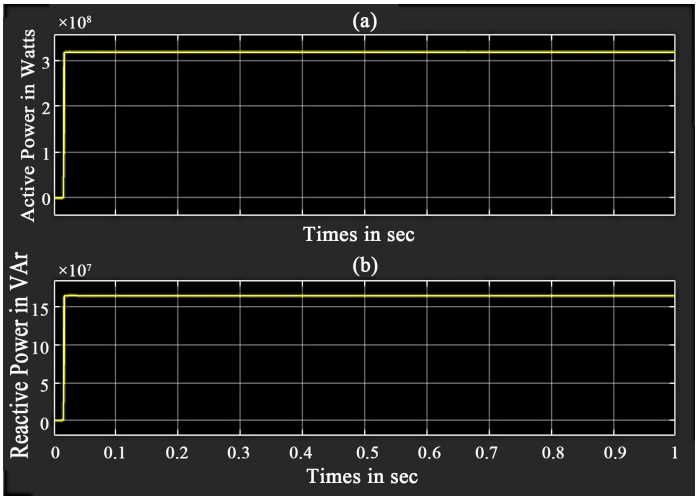

Figure 7. (a) Active power in Watts and (b) Reactive power at point A the Inga dispersal station (HV line inlet).

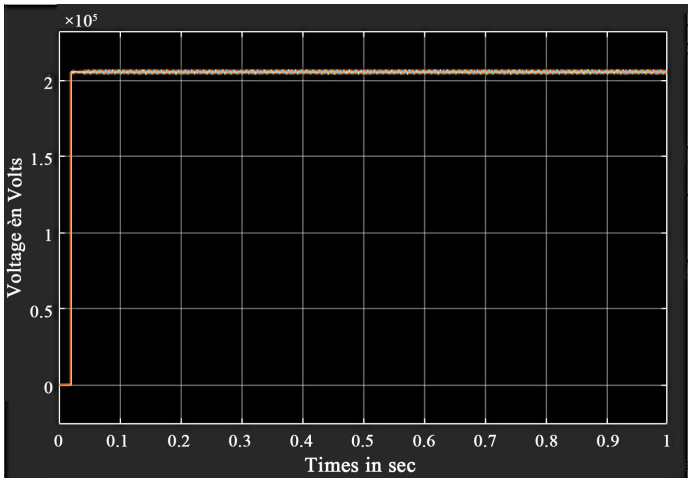

Figure 8. Voltage at point B the Kimwenza substation (220 kV HV line output) in Volts.

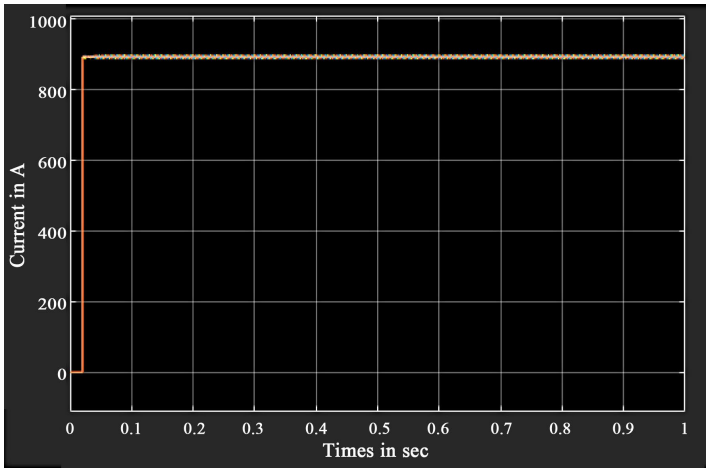

Figure 9. Current at point B at the Kimwenza substation (220 kV HV line output) in Amperes.

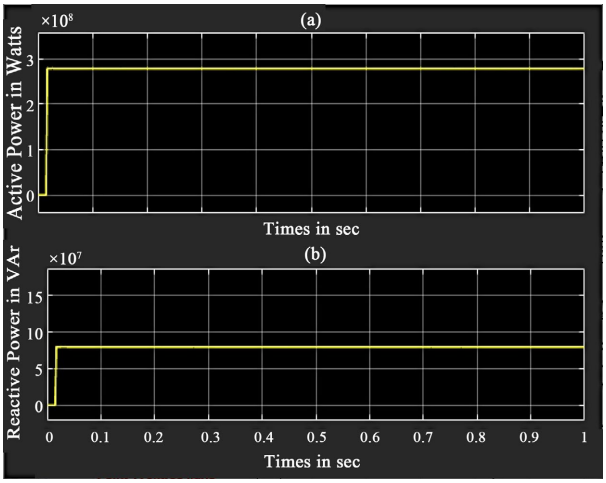

Figure 10. (a) Active power in Watts and (b) Reactive power of point B the Kimwenza substation (high-voltage line output).

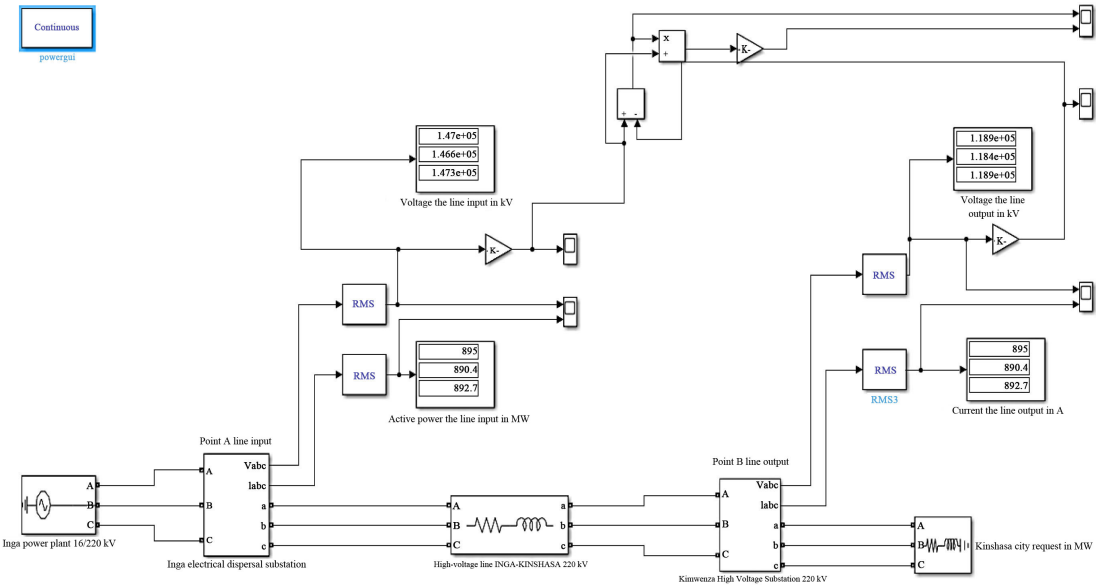

Figure 11. Simulink model of the voltage drop on the 220 kV Inga-Kimwenza high-voltage line.

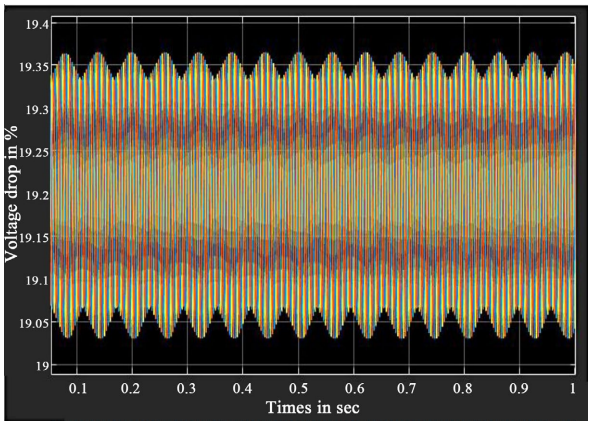

Figure 12. Voltage drop in % the end of the 220 kV Inga-Kimwenza high-voltage line.

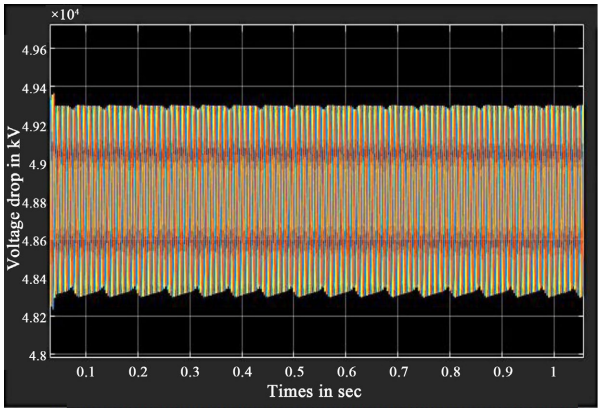

Figure 13. Voltage drop in kV the end of the 220 kV Inga-Kimwenza high-voltage line.

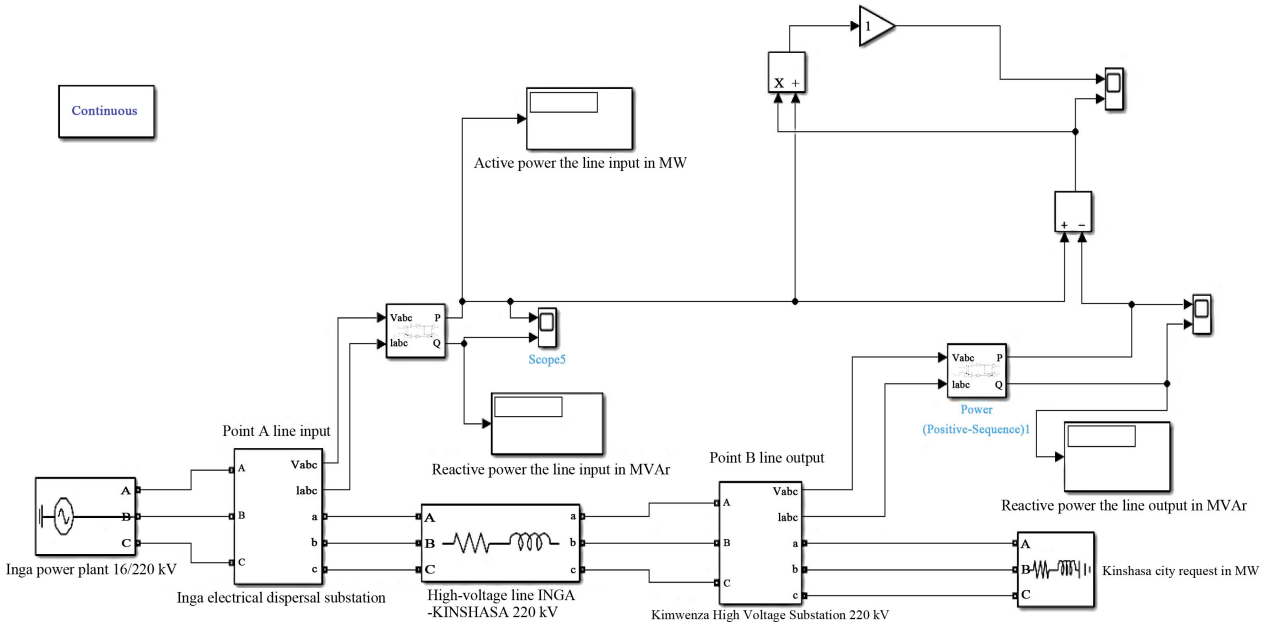

Figure 14. Simulink model of active power losses (in % and in Watts) in the 220 kV Inga-Kimwenza high-voltage line.

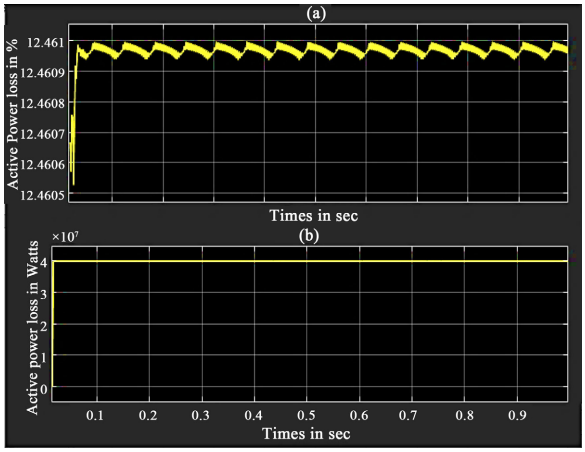

Figure 15. Results (a) active power losses in % and (b) active power losses in Watts in the 220 kV HV line obtained from the Simulink model.

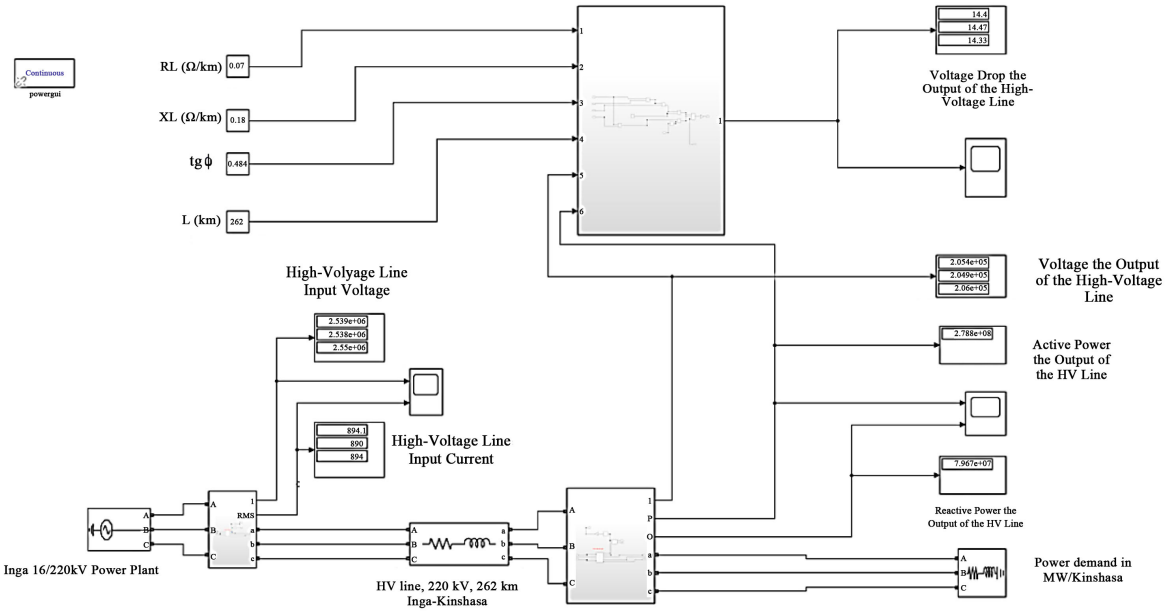

Figure 16. Model of the equation $\Delta U_r = \frac{\sqrt{3}R_L U_L I_L \cos\varphi}{U_L^2}\left(1+\frac{X_L}{R_L}\mathrm{tg}\varphi\right)$ (57) proposed for calculating the voltage drop on the HV line.

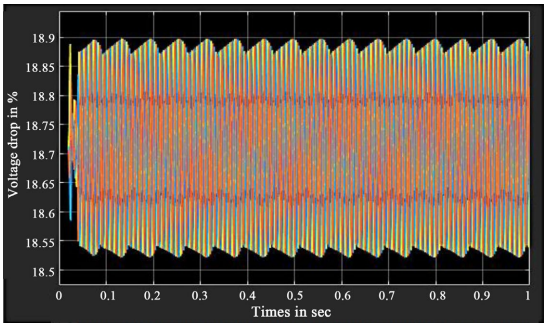

Figure 17. Results of the equation model $\Delta U_r = \frac{\sqrt{3}R_L U_L I_L \cos\varphi}{U_L^2}\left(1+\frac{X_L}{R_L}\mathrm{tg}\varphi\right)$ (57) proposed for calculating the voltage drop in % on the HV line.

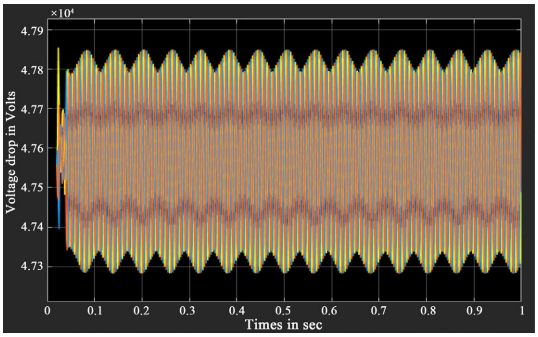

Figure 18. Results of the equation model $\Delta U_r = \frac{\sqrt{3}R_L U_L I_L \cos\varphi}{U_L^2}\left(1+\frac{X_L}{R_L}\mathrm{tg}\varphi\right)$ (57) proposed for calculating the voltage drop in Volts on the HV line.

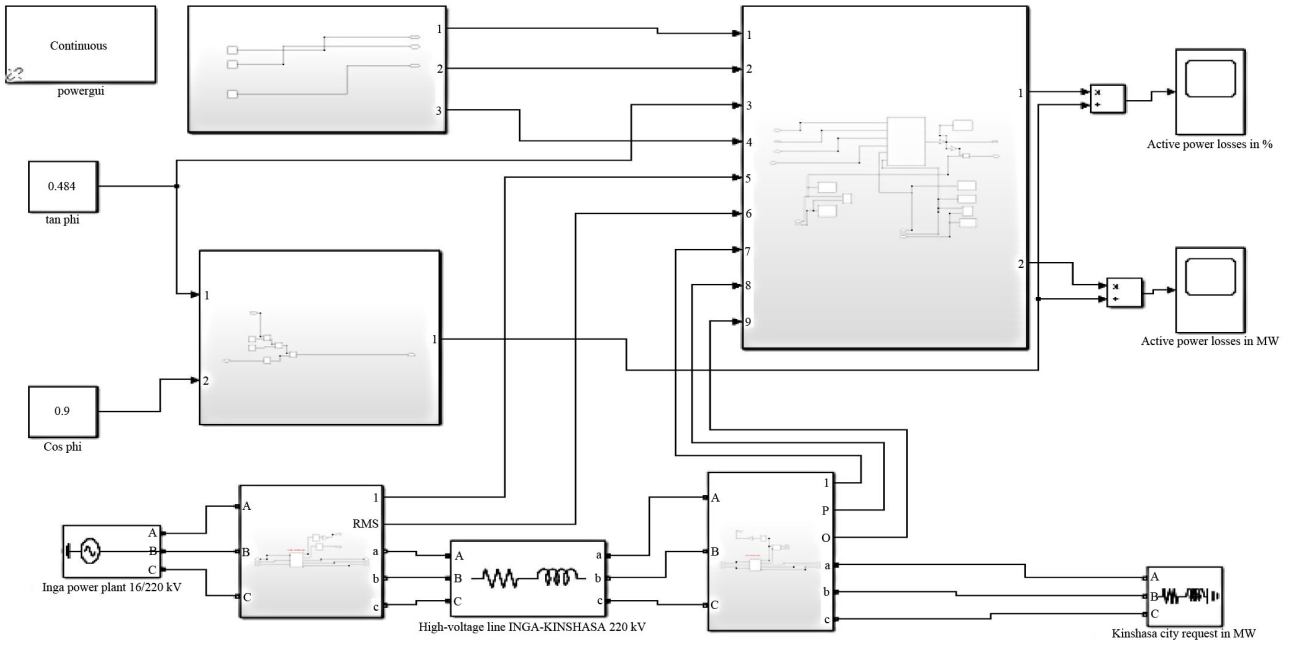

Figure 19. Proposed model (Equation (64)) for evaluating active power losses (in % and in Watts) in the HV line. Implemented in Matlab.

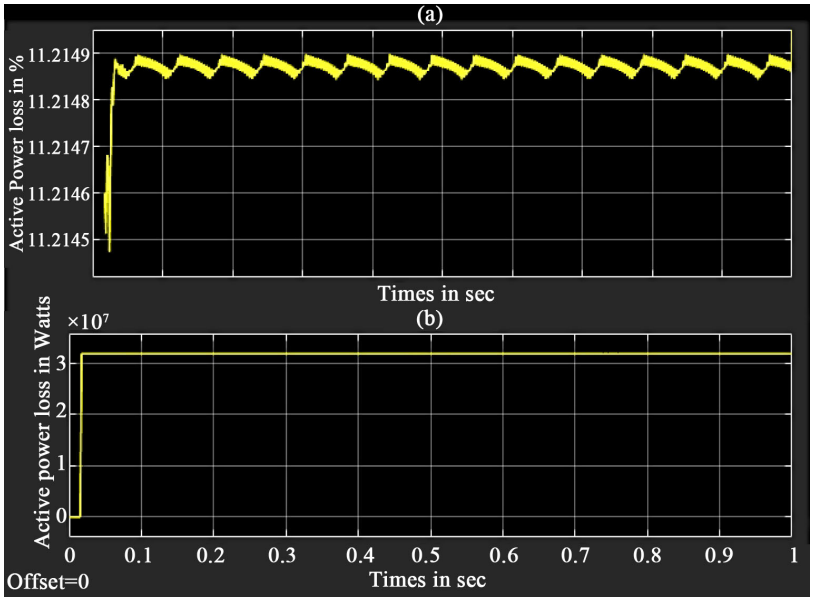

Figure 20. Results of equation 64 (a) active power losses in % and (b) active power losses in Watts in the HV line.

4. Summary of Results

Table 1. Power transmission results on the 220 kV HV line.

Settings	Simulink model	High-voltage line readings	Gap	%
High voltage input setpoint in kV	254 kV	250	4 kV	1.57%

Continued

Line current in A	894.1 A	890.1	4 A	0.45%
Operating voltage at the HV line output in kV	205.5kV	205 kV	0.5 kV	0.24%
Active power input in MW	320 MW	350 MW	30 MW	9.3%
Active power output line in MW	279 MW	275.4 MW	4.4 MW	1.5%
Reactive power input in MVAr	165.3 MVAr	169.4 MVAr	4.1 MVAr	2.5%
Reactive power output line in MVAr	79.67 MVAr	84.1 MVAr	4.43 MVAr	5.5%
Average deviation in %	-	-	-	3%

Table 2. Results of active power losses and voltage drop in the 220 kV HV line.

Settings	Simulink model	Proposed Models	Gap	%
Voltage Drop in %	19.3%	18.9%	0.4%	2%
Voltage Drop in kV	49.4 kV	47.85 kV	1.15 kV	2.3%
Active power losses in %	12.4%	11.22%	1.18%	9%
Active power losses in MW	40 MW	37 MW	3 MW	7%
Average deviation in %				5%

5. Discussions

Energy losses are of increasing concern to producers, transmission system operators, and distributors of electrical energy. Evaluating these energy losses in a high-voltage AC power system allows for the optimization of network performance, increased transmission efficiency, and reduced operating costs. Several equations exist for modeling these losses based on the characteristics of the equipment used in the installation. To obtain the results of various simulations, energy loss models based on voltage drop, derived from Maxwell's equations, were developed and used for the analytical and numerical modeling of the problem addressed in this article.

To this end, the following results were obtained:

Figure 4 represents the Simulink model of power transmission on the HV line that is the subject of our study. This figure, developed in Matlab, not only allows us to quantify the energy state of the HV line as a function of its characteristics, but also gives rise to Figures 5-10.

Figure 5 shows the voltage at the input of the high-voltage line; as we can see, this voltage is approximately 254 kV. Figure 6 shows the current drawn by the load at the end of the high-voltage line, which is 894.1 A. Figure 7(a) visualizes the profile of the active power injected at the input of the high-voltage line, which

is 320 MW, and Figure 7(b) shows the reactive power at the input of the high-voltage line, quantified at 165.3 MVAr. However, Figure 8 visualizes the voltage at the output of the high-voltage line; as we can see, this voltage is estimated at 205.5 kV. Figure 9 shows the current across the load at the end of the high-voltage line, which is 894.1 A. Figure 10(a) gives the active power profile at the output of the HV line which is 279 MW and Figure 10(b) gives the reactive power at the output of the HV line estimated at 79.67 MVAr.

We can confirm that the results in Figures 5-10 corroborate the power transmission readings provided by SNEL/DG/PKB, as shown in Table 1 above. This table indicates the discrepancies recorded between the power transmission readings provided by SNEL/DG/PKB and the Simulink model of power transmission on the HV line under study. We observe an average discrepancy of approximately 0.03, or 3%. This low root mean square error (RMSE) allows us to confirm that our results are valid.

Figure 11, developed using Matlab, presents the Simulink model of the voltage drop on the high-voltage line, which has two ends (A, the line input, and B, the output). This model yields the results shown in Figures 12-13. These figures show the voltage drops of 19.3% and 49.4 kV at the end of the line, respectively. Figure 15, also developed using Matlab, presents the Simulink model of the active power losses, expressed as a percentage and in MW, dissipated along the high-voltage line. The simulation of this model produces the results shown in Figures 15(a)-(b). These figures show that the active power losses along the line are 12.4% (see Figure 14(a)). This represents 40 MW (see Figure 15(b)). This loss rate exceeds the standard value of 5% recommended by IEC standards.

Thus, we can confirm that the results of Figures 12-13 and Figure 15 are close to those of Figures 16-20 obtained based on models 57 and 64, as can be seen in the comparison shown in Table 2 above. This table indicates the differences recorded between the results of Figures 12-13, Figure 15 and those of Figures 17-18, Figure 20. We observe an average difference of approximately 0.05, or 5%, which is within the normal range (RMSE). We can therefore confirm that our models are validated.

6. Conclusions

The electrical energy from large generating stations travels through the transmission network and then the distribution network before reaching consumers. This process results in energy losses, classified as transmission and distribution losses. This is the subject of our study. In any electrical system, energy losses are unavoidable, representing a necessary cost for transporting electricity from the point of production to the point of consumption.

To assess these energy losses, several classic methods make it possible to carry out an analysis of the energy losses produced in the electrical network; however, these classic methods do not take into account non-technical losses, have time requirements, and are cumbersome and complex in terms of the laborious calcu-

lations of numerous parameters.

Therefore, this article aimed to propose a rapid and reliable method for evaluating energy losses in high-voltage AC (HVAC) power lines, taking into account non-technical losses. The case study focused on the 220 kV Inga-Kinshasa HVAC line in the Democratic Republic of Congo, which faces numerous operational challenges. Implementing this method requires measuring the voltage drop at both ends of the HV line, which is easier and less expensive, and calculating the power factor.

The results presented in this article highlight the direct corroboration between the power transit readings provided by SNEL/DG/PKB [45] and the Simulink model of power transit on the HTAC line which is the subject of our study, with an average difference of around 0.03 or 3%, a low mean squared error according to the standard (RMSE).

Thus, we can confirm that the simulation results of voltage drop and energy losses in the HV line obtained via the Matlab environment bring the models proposed via equations 57 and 64 closer together, with an average difference of around 0.05 or 5%, which is within the margin of the standard (RMSE).

These results can be used for practical applications in the engineering and design of high-voltage transmission networks. They can also guide policymakers.

Analysis of the results of the applications processed shows that the proposed method is very useful and constitutes an adequate model for evaluating these energy losses in HTAC power lines.

The prospects arising from this study of energy loss analysis and modelling are vast, ranging from the optimization of transformers and motors to the design of absorbent materials, including improving the efficiency of electrical networks and analyzing electromagnetic compatibility, to reduce energy waste in numerous technological and industrial sectors. In addition, the study assesses the robustness of the proposed models.

A compact validation step at several operating points (e.g., different load levels or time windows) and a consistent definition of the error measurement (e.g., RMSE/MAE with units and normalization) so that agreement is not demonstrated on a single representative case, sensitivity control for parameters that most affect losses (especially conductor resistance as a function of temperature and assumed power factor) and estimation of losses change in case of plausible parameter variation to support robustness claims, will be the subject of future studies.

Conflicts of Interest

The authors declare no conflicts of interest regarding the publication of this paper.

References

[1] Belahcen, A., *et al.* (2020) Coupled Magneto-Mechanical Analysis of Iron Sheets Under Biaxial Stress. *IEEE Transactions on Magnetics*. https://www.researchgate.net/publication/283320821_Coupled_Magneto-Mechanical_Analysis_of_Iron_Sheets_Under_Biaxial_Stress#:~:text=Abstract%20and%20Figures,vector%20potential%20in%20the%20sample

[2] Yan, X., Yu, X., Shen, M., Xie, D. and Bai, B. (2016) Research on Calculating Eddy-Current Losses in Power Transformer Tank Walls Using Finite-Element Method Combined with Analytical Method. *IEEE Transactions on Magnetics*, **52**, 1-4. https://doi.org/10.1109/tmag.2015.2494375

[3] Elizondo, D., Barrios, E.L., Sanchis, P. and Ursua, A. (2020). Analytical Modeling of High-Frequency Winding Loss in Round-Wire Toroidal Inductors. 2020 IEEE 21st Workshop on Control and Modeling for Power Electronics (COMPEL), Aalborg, 9-12 November 2020. https://doi.org/10.1109/compel49091.2020.9265782

[4] Aninye, A., *et al*. (2017) Analysis of Losses in Power Transformer. *American Journal of Electrical and Electronic Engineering*, **5**, 94-101.

[5] Bíró, O., Preis, K. and Ticar, I. (2005) A FEM Method for Eddy Current Analysis in Laminated Media. *COMPEL—The International Journal for Computation and Mathematics in Electrical and Electronic Engineering*, **24**, 241-248. https://doi.org/10.1108/03321640510571264

[6] De Gersem, H., Vanaverbeke, S. and Samaey, G. (2012) Three-Dimensional-Two-Dimensional Coupled Model for Eddy Currents in Laminated Iron Cores. *IEEE Transactions on Magnetics*, **48**, 815-818. https://doi.org/10.1109/tmag.2011.2172924

[7] Kelemen, F., Strac, L. and Berberovic, S. (2008) Estimation of Stray Losses Outside of Windings in Power Transformers Using Three Dimensional Static Magnetic Field Solution and Statistics. 2008 18*th International Conference on Electrical Machines*, Vilamoura, 6-9 September 2008, 1-3. https://doi.org/10.1109/icelmach.2008.4800066

[8] Hollaus, K. and Schöberl, J. (2015) Multi-Scale FEM and Magnetic Vector Potential a for 3D Eddy Currents in Laminated Media. *COMPEL—The International Journal for Computation and Mathematics in Electrical and Electronic Engineering*, **34**, 1598-1608. https://doi.org/10.1108/compel-02-2015-0090

[9] Hollaus, K. and Schoberl, J. (2018) Some 2-D Multiscale Finite-Element Formulations for the Eddy Current Problem in Iron Laminates. *IEEE Transactions on Magnetics*, **54**, 1-16. https://doi.org/10.1109/tmag.2017.2777395

[10] Kaimori, H., Kameari, A. and Fujiwara, K. (2007) FEM Computation of Magnetic Field and Iron Loss in Laminated Iron Core Using Homogenization Method. *IEEE Transactions on Magnetics*, **43**, 1405-1408. https://doi.org/10.1109/tmag.2007.892429

[11] Liew, M.C. and Bodger, P.S. (2001) Partial-Core Transformer Design Using Reverse Modelling Techniques. *IEE Proceedings—Electric Power Applications*, **148**, 513-519. https://doi.org/10.1049/ip-epa:20010587

[12] Laffont, M. (2009) Perte d'énergie dans les réseaux de distribution d'électricité. https://mathiaslaffont.wordpress.com/wp-content/uploads/2011/01/rdv-tel-27_04_091.pdf

[13] Frljić, S., Trkulja, B. and Drandić, A. (2023) Eddy Current Losses in Power Voltage Transformer Open-Type Cores. *COMPEL—The International Journal for Computation and Mathematics in Electrical and Electronic Engineering*, **42**, 1039-1051. https://doi.org/10.1108/compel-01-2023-0016

[14] Muhammad, S.S., Abdulrazak, S., Bakare, G.A., Abdulhafiz, S. and Nazif, D.M. (2025) Modelling and Analysis of a Power Transformer Using Finite Element Analysis. *Asian Journal of Science, Technology, Engineering, and Art*, **3**, 902-920. https://doi.org/10.58578/ajstea.v3i3.5703

[15] Kolar, J.W. and Huber, J.E. (2021) The DNA of Future High Performance Power Electronic Systems. Swiss Federal Institute of Technology (ETH) Zurich Power Electronic Systems Laboratory.

[16] Cao, X. (2023) New Insights into Maxwell's Equations Based on New Experimental Discoveries. *Composites Communications*, **39**, Article ID: 101552. https://doi.org/10.1016/j.coco.2023.101552

[17] Huang, X., Li, Q., Liu, Z. and Lee, F.C. (2014) Analytical Loss Model of High Voltage Gan HEMT in Cascode Configuration. *IEEE Transactions on Power Electronics*, **29**, 2208-2219. https://doi.org/10.1109/tpel.2013.2267804

[18] Lahcen, B.H. (2019) Minimization of Active Losses in an Electrical Network Using the Particle Swarm Optimization Algorithm. Master's Thesis, Université Kasdi Merbah Ouargla. https://dspace.univ-ouargla.dz/jspui/bitstream/123456789/21766/1/Minimisation%20des%20pertes%20actives%20dans%20un%20r%C3%A9seau%20%C3%A9lectrique%20par%20l%E2%80%99algorithme%20d%E2%80%99optimisation%20par%20essaim%20de%20particules.pdf

[19] Saad, H.A. (2015) Modeling and Simulation of a VSCMMC Type HVDC Link. Poly-Publie. https://publications.polymtl.ca/1699/

[20] Boukaroura, A., Slimani, L. and Bouktir, T. (2021) Contribution to the Modeling and Optimization of Distribution Networks under Uncertainties. Ph.D. Thesis, Larbi Ben M'hidi-Oum El Bouaghi University. https://www.researchgate.net/publication/366811763_Contribution_a_la_modelisation_et_a_l'optimisation_des_reseaux_de_distribution_sous_incertitudes

[21] PRISME (2012) Les pertes techniques dans les réseaux de transport et de distribution de l'électricité. La Planification Energétique Sectorielle Fiche Nº 8, https://www.ifdd.francophonie.org/wp-content/uploads/2021/09/469_2012_PertesTech-8-1.pdf

[22] Babiker, A.K.M., Ahmad, S., Ahmed, I. and Khalid, M. (2025) Optimal Power Flow: A Review of State-of-the-Art Techniques and Future Perspectives. *IEEE Access*, **13**, 60012-60039. https://doi.org/10.1109/ACCESS.2025.3556168

[23] Kovernikova, L.I. and Bui, N.H. (2024) Additional Power Losses under Non-Sinusoidal Conditions in a 22 kV Overhead Power Line. *Energy Systems Research*, **7**, 31-36. https://doi.org/10.25729/esr.2024.01.0003

[24] Al Ameri, A. (2017) Analytical Study Methods for Reducing Power Losses in Meshed Electrical Networks Using Optimization Techniques for the Sizing and Location of Decentralized Generators. Ph.D. Thesis, University of Le Havre. https://theses.hal.science/tel-01623691v1

[25] Ofuyekpone, O.D., Okoubulu, A.B., Eduviere, O.G. and Naenwi, Y. (2026) Dynamic Loss Assessment of HVAC and HVDC Transmission Systems under High-Penetration Renewable Power Integration: A Novelty Approach. *International Journal of Research and Scientific Innovation*, **13**, 309-321. https://doi.org/10.51244/ijrsi.2026.1303000029

[26] Zhang, F., *et al*. (2022) High-Voltage Cable Energy Loss Calculation and Optimization. *IET Generation*, *Transmission & Distribution*, **16**, 2045-2058.

[27] Cevallos, D., Barrera-Singaña, C. and Arcos, H. (2025) Optimal Adjustment of Reactive Power in Transmission Systems by Variation of Taps in Static Elements Using the Mean-Variance Mapping Optimization Algorithm. *Energies*, **18**, Article 2141. https://doi.org/10.3390/en18082141

[28] Baviskar, A., Das, K. and Hansen, A.D. (2021) Minimize Distribution Network Losses Using Wind Power. *IET Conference Proceedings*, **2021**, 1954-1958. https://doi.org/10.1049/icp.2021.2143

[29] Kiangebeni Lusimbakio, K., Boketsu Lokanga, T., Sedi Nzakuna, P., Paciello, V., Nzuru Nsekere, J. and Tshimanga Tshipata, O. (2025) Evaluation of the Impact of Photovoltaic Solar Power Plant Integration into the Grid: A Case Study of the Western Transmission Network in the Democratic Republic of Congo. *Energies*, **18**, Article 639. https://doi.org/10.3390/en18030639

[30] Wu, X., Yang, C., Han, G., Ye, Z. and Hu, Y. (2022) Energy Loss Reduction for Distribution Networks with Energy Storage Systems via Loss Sensitive Factor Method. *Energies*, **15**, Article 5453. https://doi.org/10.3390/en15155453

[31] Goop, J., Odenberger, M. and Johnsson, F. (2016) Distributed Solar and Wind Power—Impact on Distribution Losses. *Energy*, **112**, 273-284. https://doi.org/10.1016/j.energy.2016.06.029

[32] Al Ameri, A., Ounissa, A., Nichita, C. and Djamal, A. (2017) Power Loss Analysis for Wind Power Grid Integration Based on Weibull Distribution. *Energies*, **10**, Article 463. https://doi.org/10.3390/en10040463

[33] MuniSekhar, P., Jayakrishna, G. and Visali, N. (2019) Optimal Sizing and Placement of ESS in Distribution System with Renewable Energy Integration Using Multi-Objective Hybrid Optimization Technique. 2019 2*nd International Conference on Power and Embedded Drive Control* (*ICPEDC*), Chennai, 21-23 August 2019, 81-86. https://doi.org/10.1109/icpedc47771.2019.9036604

[34] Cao, J., Du, W., Wang, H.F. and Bu, S.Q. (2013) Minimization of Transmission Loss in Meshed AC/DC Grids with VSC-MTDC Networks. *IEEE Transactions on Power Systems*, **28**, 3047-3055. https://doi.org/10.1109/tpwrs.2013.2241086

[35] Yongfei, M. and Wang, X. (2024) Research on the Impact of Electric Vehicle Access on Distribution Network Loss. 2024 6*th International Conference on Energy Systems and Electrical Power* (*ICESEP*), Wuhan, 21-23 June 2024, 917-921. https://doi.org/10.1109/icesep62218.2024.10651660

[36] Díaz, S., *et al*. (2021) Electric Power Losses in Distribution Networks. *Turkish Journal of Computer and Mathematics Education* (*TURCOMAT*), **12**, 581-591. https://www.researchgate.net/publication/351879877_Electric_power_losses_in_distribution_networks

[37] Nguyen, T.T., Dinh, B.H., Pham, T.D. and Nguyen, T.T. (2020) Active Power Loss Reduction for Radial Distribution Systems by Placing Capacitors and PV Systems with Geography Location Constraints. *Sustainability*, **12**, Article 7806. https://doi.org/10.3390/su12187806

[38] Chetia, A. (2025) Artificial Intelligence for Determining Transmission and Distribution Loss Reduction for Electrical Systems: A Comprehensive Framework. Department of Energy Tezpur University. https://www.researchgate.net/publication/398258443_ARTIFICIAL_INTELLIGENCE_FOR_DETERMINING_TRANSMISSION_AND_DISTRIBUTION_LOSS_REDUCTION_FOR_ELECTRICAL_SYSTEMS_A_COMPREHENSIVE_FRAMEWORK

[39] Lontchi, C.M. (2021) Contribution to the Prediction of Power Losses on an Electrical Network Using a Neural Network-Based Model. Master's Degree, University of Quebec at Montreal. https://archipel.uqam.ca/16071/1/M17363.pdf

[40] Fateh, B. (2019) Optimal Distribution of Energy Flows and Impact on the Performance of a High-Voltage Electrical System. Ph.D. Thesis, Université 8 Mai 1945 Guelma. https://dspace.univ-guelma.dz/jspui/handle/123456789/3674

[41] Mancer, N., Mahdad, B., Srairi, K. and Hamed, M. (2012) Minimizing Power Transmission Losses Through the Use of Global Optimization Methods. 7*th International*

Conference on Electrical Engineering, Batna Alger, 8-10 October 2012. https://www.researchgate.net/publication/283706566_Minimisation_des_Pertes_de_Transmission_d'Energie_par_Utilisation_des_Methodes_Globales_d'Optimisation

[42] Tchuidjan, R., *et al*. (2011) Reduction of Power Losses in a Distribution Network Supplied by a New and Renewable Energy Generator. *Renewable Energy Review*, **14**, 449-459. https://asjp.cerist.dz/en/article/120161

[43] Oloulade, A., *et al*. (2018) Multi-Criteria Optimization of D-STATCOM Placement in a Distribution Network by Ant Colonies. Electrical Engineering Symposium. https://hal.science/hal-02983369/document

[44] Djedidi, I. (2023) Optimisation Des Performances Du Réseau Électrique de Distribution Par Des Méthodes Évolutionnaires. Ph.D. Thesis, Université Mohamed Khider Biskra. http://thesis.univ-biskra.dz/6257/

[45] Shaikh, S., Arif, A. and Aman, M.M. (2023) Estimation of Technical Losses on Transmission Systems Using a Neural Network Prognosis Algorithm (NNPA). *Engineering Proceedings*, **46**, Article 25. https://doi.org/10.3390/engproc2023046025

[46] Said, A.H. (2018) Integration of Storage into Low-Voltage Electrical Network Planning Methods. Ph.D. Thesis, Grenoble Alpes University. https://theses.hal.science/tel-01841465/

[47] Salhi, A. (2012) Optimal Planning of Electrical Energy Exchange between Interconnected Networks. Master's Thesis, University Mohamed Khider Biskra. http://thesis.univ-biskra.dz/1621/